EUROPEAN ORGANIZATION FOR NUCLEAR RESEARCH

L3 Note 2567
June 30, 2000

Preliminary Results on the Measurement of Triple-Gauge-Boson Couplings of the W Boson at LEP

The L3 Collaboration

Abstract

We report preliminary results on the measurement of triple-gauge-boson couplings of the W boson in e^+e^- collisions at $192 \le \sqrt{s} \le 202$ GeV. Using W-pair events selected in a data sample corresponding to a total luminosity of 233.25 pb^{-1} collected by the L3 detector at LEP during the 1999 data taking period, we measure the couplings g_1^{Z}, κ_γ, λ_γ, g_5^{Z}, λ_{Z} and κ_{Z}. Preliminary results are combined with our previous W-pair results based on the data collected in 1998 and with results obtained from the study of single-W production. We also show results of the measurement of the electromagnetic couplings κ_γ and λ_γ, obtained analysing the single-photon production in the same data sample.

Submitted to the *XXXth International Conference on High Energy Physics*
July 27 - August 2, 2000, Osaka, Japan

1 Introduction

For the 1999 data taking period, the centre-of-mass energy, $\sqrt{s}$, of the e^+e^- collider LEP at CERN started at 192 GeV and was increased in three steps up to 202 GeV. These energies are well above the kinematic threshold of W-boson pair production, $e^+e^- \rightarrow W^+W^-$.

W-pair production, single-W production ($e^+e^- \rightarrow We\nu$) and single-photon production ($e^+e^- \rightarrow \nu\bar{\nu}\gamma$) all depend on the trilinear self couplings among the electroweak gauge bosons [1]. The existence of triple-gauge-boson vertices γWW and ZWW is predicted in the Standard Model as a consequence of the non-Abelian gauge structure of the electroweak theory [2]. To lowest order within the Standard Model, three Feynman diagrams contribute to W-pair production, the s-channel γ and Z-boson exchange and the t-channel ν_e exchange, referred to as CC03 [3–5].

At present centre-of-mass energies, single-W production is sensitive to the electromagnetic gauge couplings only. The γWW vertex appears in one of the contributing t-channel Feynman diagrams in W$e\nu$ production, and dominates the corresponding diagram containing the ZWW vertex. Radiation of a photon from the t-channel exchanged W boson in the process $e^+e^- \rightarrow \nu_e\bar{\nu}_e$ becomes significant for centre-of-mass energies far above the Z pole and involves as well the γWW vertex.

In general the vertices γWW and ZWW are parametrised in terms of seven complex triple-gauge-boson couplings (TGC) each [6], too many to be measured simultaneously. Regarding only C- and P-conserving couplings, and assuming electromagnetic gauge invariance, a total of five couplings remain: g_1^Z, κ_γ, λ_γ, κ_Z and λ_Z, which have at tree level within the Standard Model the values $g_1^Z = \kappa_\gamma = \kappa_Z = 1$, while $\lambda_\gamma = \lambda_Z = 0$. A further reduction in number of couplings can be made by assuming custodial SU(2) symmetry, leading to the constraints $\Delta\kappa_Z = \Delta g_1^Z - \Delta\kappa_\gamma \tan^2\theta_w$ and $\lambda_Z = \lambda_\gamma$, where θ_w is the weak mixing angle [7–10] and Δ denotes the difference of these couplings with respect to the Standard Model value. When these constraints are applied, these couplings are related to the α couplings used in our previous publications [11, 12] by linear transformations [1)]. These couplings correspond to the operators in a linear realization of a gauge invariant effective Lagrangian that do not affect the gauge boson propagators at tree level [10]. Besides these couplings, another CP-conserving coupling (but not C- and P- separately) exists in the above mentioned parametrisation, namely g_5^Z, which has the value of zero at tree level within the Standard Model.

In this note we report on the determination of these triple-gauge-boson couplings of the W boson, based on WW events selected from the large data sample collected in the year 1999 at the following four average centre-of-mass energies: 191.60 (hereafter called 192) GeV, 195.54 (196) GeV, 199.54 (200) GeV and 201.75 (202) GeV, corresponding to integrated luminosities of respectively 29.72 pb^{-1}, 83.69 pb^{-1}, 82.80 pb^{-1} and 37.04 pb^{-1}, which means a total luminosity of 233.25 pb^{-1}. The couplings are determined based on total and multi-differential cross sections. These preliminary results based on the 1999 data are combined with our previous results based on 1998 [13] data collected at a centre-of-mass energy of 188.7 (189) GeV, and with the results of the measurement of the electromagnetic couplings (κ_γ and λ_γ) based on single-W production at the same centre-of-mass energies. The single-W analysis is described elsewhere [14, 15]; In this note we will only describe the combination procedure. Results will also be reported for the analysis of single-photon production, which is sensitive to the electromagnetic couplings κ_γ and λ_γ.

In W-pair, single-W and single-photon production, the triple-gauge-boson vertices are tested

[1)] These transformations are: $\alpha_{W\Phi} = \Delta g_1^Z \cos^2\theta_w$, $\alpha_{B\Phi} = \Delta\kappa_\gamma - \Delta g_1^Z \cos^2\theta_w$, and $\alpha_W = \lambda_\gamma$.

at different momentum-transfer scales Q^2: $Q^2 = s$ for W-pair production, $Q^2 = M_{\mathrm{W}}^2$ for single-W production, and $Q^2 = 0$ for single-photon production. Compared to the current level of statistical accuracy, the Q^2 dependence of the TGCs expected in the Standard Model is negligible [6] and is thus ignored in the combination.

2 Analysis

2.1 W-pair events

The L3 detector is described in detail in Reference 16. The event selections used in this analysis are identical to those described in Reference 17. These selections reconstruct the visible fermions in the final state, *i.e.*, electrons, muons, τ jets corresponding to the visible τ decay products, and hadronic jets corresponding to quarks [11,18]. A kinematic fit is then performed to improve the resolution in the measured fermion energies and angles and to determine those not measured [12]. Four-momentum conservation and equal mass of the two W bosons are imposed as constraints. In $qq\tau\nu$ events, the energies of the two hadronic jets are rescaled by a common factor so that their sum equals half the centre-of-mass energy. In $qqqq$ events, jets are paired to W's following the criterion of smallest mass difference between the W candidates, after first disregarding the combination with the smallest sum of masses. On Monte Carlo events, this pairing is found to be correct for 73% of all selected $qqqq$ events with $192 \leq \sqrt{s} \leq 202$ GeV.

Selection efficiencies and background contaminations of all processes are determined by Monte Carlo simulations. The following Monte Carlo event generators are used to simulate the signal and background reactions: KORALW [19] and HERWIG [20] ($\mathrm{e^+e^-} \rightarrow \mathrm{WW} \rightarrow ffff(\gamma)$); EXCALIBUR [21] ($\mathrm{e^+e^-} \rightarrow ffff(\gamma)$); PYTHIA [22] ($\mathrm{e^+e^-} \rightarrow q\bar{q}(\gamma), \mathrm{ZZ}(\gamma)$); KORALZ [23] ($\mathrm{e^+e^-} \rightarrow \mu^+\mu^-(\gamma),\ \tau^+\tau^-(\gamma)$); BHAGENE3 [24], BHWIDE [25] and TEEGG [26] ($\mathrm{e^+e^-} \rightarrow \mathrm{e^+e^-}(\gamma)$), DIAG36 [27] and LEP4F [28] (leptonic two-photon collisions); PHOJET [29] (hadronic two-photon collisions). The response of the L3 detector is modeled with the GEANT [30] detector simulation program which includes the effects of energy loss, multiple scattering and showering in the detector materials and in the beam pipe.

Fixing the mass of the W boson [31] and neglecting photon radiation and final-state fermion helicities, five phase-space angles completely describe the four-fermion final state for unpolarised initial states. These are the polar angle of the W^- boson, $\cos\Theta_{\mathrm{W}}$, and the polar and azimuthal decay angles in the rest systems of the two decaying W bosons, $\cos\theta^*_\pm$ and $\phi^*_\pm$, for the fermion and antifermion in W^- and W^+ decay, respectively.

For charged leptons, the sign of their electric charge determines whether they are fermions or antifermions. For hadronic jets, the flavour and charge of the original quark is not measured. Thus, there arises a two-fold ambiguity in the decay angles of hadronically decaying W bosons, $(\cos\theta^*_q, \phi^*_q) \leftrightarrow (-\cos\theta^*_q, \pi + \phi^*_q)$. If both W bosons decay hadronically, the polar angle of the W^- boson also has a two-fold ambiguity, $\cos\Theta_{\mathrm{W}} \leftrightarrow -\cos\Theta_{\mathrm{W}}$. This ambiguity is resolved by combining the jet charges of each pair of jets to determine the charge of each W. The difference in the two W charges is then used to determine the sign of $\cos\Theta_{\mathrm{W}}$. The charge of each jet is determined from a rapidity weighted sum of the tracks reconstructed in the central tracking chamber and assigned to the jet with rapidity weight $\kappa = 0.5$ [32,33]. The sign assignment is found to be correct in 71% of the events with $192 \leq \sqrt{s} \leq 202$ GeV, if the jets are correctly paired. The resolutions in these phase-space angles, after applying the kinematic fit imposing the equal mass constraint, are shown in Figure 1.

The triple-gauge-boson couplings are determined using a maximum likelihood fit. The fit considers a set of values of reconstructed phase space angles Ω for each data event. The data are treated as unbinned; the total likelihood is the product of the normalised differential cross section, $L(\Omega, \Psi)$, for all data events. For a given four-fermion final state i, one has:

$$L_i(\Omega_i, \Psi) \quad = \quad \frac{1}{\sigma_i(\Psi) + \sigma_i^{\mathrm{BG}}} \left[\frac{\mathrm{d}\sigma_i(\Omega_i, \Psi)}{\mathrm{d}\Omega_i} + \frac{\mathrm{d}\sigma_i^{\mathrm{BG}}(\Omega_i)}{\mathrm{d}\Omega_i} \right] ,$$

where σ_i and σ_i^{BG} are the accepted signal and background cross sections. The total and differential cross sections of the accepted background are independent of the triple-gauge-boson couplings Ψ. They are taken directly from Monte Carlo simulations.

The total and differential signal cross sections depend on Ψ. For values Ψ_{fit} varied during the fitting procedure, they are determined by a reweighting procedure applied to Monte Carlo events originally generated with parameter values Ψ_{gen}. The event weights R_i are calculated as the ratio:

$$R_i(p_1, p_2, p_3, p_4, k_\gamma, \Psi_{\mathrm{fit}}, \Psi_{\mathrm{gen}}) \quad = \quad \frac{\left| \mathcal{M}_i^{\mathrm{4F}}(p_1, p_2, p_3, p_4, k_\gamma, \Psi_{\mathrm{fit}}) \right|^2}{\left| \mathcal{M}_i^{\mathrm{CC03}}(p_1, p_2, p_3, p_4, k_\gamma, \Psi_{\mathrm{gen}}) \right|^2} ,$$

where $\mathcal{M}_i$ is the matrix element of the four-fermion final state i. The matrix elements are calculated for the generated four-vectors, $(p_1, p_2, p_3, p_4, k_\gamma)$, of the four fermions and any radiative photons in the event. Since the Monte Carlo sample used for reweighting is based on the three Feynman graphs in W-pair production (CC03), the matrix element in the denominator is calculated using only CC03 graphs. The matrix element in the numerator is based on all tree-level graphs contributing to the four-fermion final state i. The calculation of matrix elements is done with the EXCALIBUR [21] [2)] event generator. The total accepted signal cross section for a given set of parameters Ψ_{fit} is then:

$$\sigma_i(\Psi_{\mathrm{fit}}) \quad = \quad \frac{\sigma_i^{\mathrm{gen}}}{N_i^{\mathrm{gen}}} \cdot \sum_j R_i(j, \Psi_{\mathrm{fit}}, \Psi_{\mathrm{gen}}) ,$$

where σ_i^{gen} denotes the cross section corresponding to the total Monte Carlo sample containing N_i^{gen} events. The sum extends over all accepted Monte Carlo events j. The accepted differential signal cross section in reconstructed quantities Ω_i is determined by averaging Monte Carlo events inside a box in Ω_i around each data event [34]:

$$\frac{\mathrm{d}\sigma_i(\Omega_i, \Psi_{\mathrm{fit}})}{\mathrm{d}\Omega_i} \quad = \quad \frac{\sigma_i^{\mathrm{gen}}}{N_i^{\mathrm{gen}}} \cdot \frac{1}{\Delta_i^\Omega} \sum_{j \epsilon \Delta_i^\Omega} R_i(j, \Psi_{\mathrm{fit}}, \Psi_{\mathrm{gen}}) ,$$

where Δ_i^Ω is the volume of the box and the sum extends over all accepted Monte Carlo events j inside the box. This method takes Ω_i-dependent detector effects and Ψ-dependent efficiencies and purities properly into account.

In addition, extended maximum likelihood fits are performed by including the overall normalisations according to the measured total W-pair cross sections. The likelihood is multiplied by the Poissonian probabilities to obtain the numbers of events observed in the data [11, 18]

[2)] EXCALIBUR uses the couplings δ_{Z}, x_γ, y_γ, x_{Z}, y_{Z} and z_Z defined in Reference 8. These couplings are related to the couplings used in this note by the relations $\Delta\kappa_\gamma = x_\gamma$, $\lambda_\gamma = y_\gamma$, $\Delta g_1^{\mathrm{Z}} = \delta_{\mathrm{Z}} \tan\theta_w$, $\Delta\kappa_{\mathrm{Z}} = (\delta_{\mathrm{Z}} + x_{\mathrm{Z}}) \tan\theta_w$, $\lambda_{\mathrm{Z}} = y_{\mathrm{Z}} \tan\theta_w$ and $g_5^{\mathrm{Z}} = -\frac{s}{M_W^2} z_Z \tan\theta_w$ where θ_w is the weak mixing angle, M_W the W mass and s the square of the centre-of-mass energy.

given the integrated luminosities and the expectations for the total accepted signal and background cross sections, $\sigma_i(\Psi_{\text{fit}})$ and σ_i^{BG}, at all centre-of-mass energies.

The fit method described above determines the parameters without any bias as long as the Monte Carlo describes photon radiation (ISR) and detector effects such as resolution and acceptance functions correctly. By fitting large Monte Carlo samples, typically a hundred times the data, the fitting procedure is tested to high accuracy. The fits reproduce well the values of the parameters of the large Monte Carlo samples being fitted. Also, the fit results do not depend on the values of the parameters Ψ_{gen} of the Monte Carlo sample subjected to the reweighting procedure.

Data taken at $\sqrt{s} = 192$ GeV, 196 GeV, 200 GeV and 202 GeV are combined in a single fit. The combination with the results from 189 GeV data are obtained by adding the likelihood curves. For all the energies the differential cross section is used as well as the total cross section. In the calculation of the likelihood from the total cross section, all final states are used. For the differential cross section for semileptonic $qq\ell\nu$ events, the variables considered in the fit are $\cos\Theta_{\text{W}}$ and the decay angles of the leptonically decaying W boson, $\cos\theta_l^*$ and ϕ_l^*; for fully hadronic $qqqq$ events, only $\cos\Theta_{\text{W}}$ is used. From the data taken at $192 \leq \sqrt{s} \leq 202$ GeV, a total of 1330 $qq\ell\nu$ events enter in the fit (485 $qqe\nu$ events, 416 $qq\mu\nu$ events and 429 $qq\tau\nu$ events for which the τ charge is determined), whereas 1850 hadronic $qqqq$ events are used for which $\cos\Theta_{\text{W}}$ is determined. The distributions of these phase-space angles are shown in Figure 2. For total cross sections, the EXCALIBUR predictions are scaled to match the GENTLE predictions to account for the more complete calculation of radiative corrections by GENTLE.

2.2 Single-W events

If in the process $\text{e}^+\text{e}^- \to \text{We}\nu$ the final state electron is scattered at low polar angles, it escapes detection along the beam pipe. Only the decay products of a single W boson are observed.

Leptonic single-W events, where the W boson decays into a lepton-neutrino pair, are selected by requiring a single charged lepton, either electron, muon or τ jet, without any other activity in the detector [14, 15]. Hadronic single-W events, where the W boson decays into a quark pair, are selected by requiring the presence of two acoplanar hadronic jets, no leptons, and large transverse momentum imbalance. After a preselection, several kinematic variables are fed into a neural network trained to separate better the hadronic single-W events from the dominating background of $qq\ell\nu$ W-pair events. The total cross section and the distribution of the neural-network output variable are used in the determination of triple gauge couplings.

Some of the hadronic single-W events are also selected by the $qq\ell\nu$ W-pair selections, mainly $qq\tau\nu$ events. In order to avoid double counting, such events are considered in the W-pair sample only.

This reduces the sensitivity of the single-W sample to the couplings as compared to the sensitivity obtained in the single-W TGC analysis [14, 15]. However, in combination with the W-pair signal the overall sensitivity is expected to be better than that achieved when removing the duplicate events from the $qq\ell\nu$ W-pair samples.

2.3 Single-Photon Events

Single-photon events are selected by requiring one energy deposition above 5 GeV inside a polar angular range from 14° to 166° in the electromagnetic calorimeter with an electromagnetic shower shape and without any other activity in the detector [35]. The KORALZ [36] Monte

Carlo generator is used to model the $e^+e^- \rightarrow \nu\bar{\nu}\gamma\gamma$ process according to the SM. We select 572 events at $\sqrt{s} = 189$ GeV and 665 events at $\sqrt{s} = 192-202$ GeV compared to a SM expectation of 567.3 and 672.4 events respectively. Figure 3 shows the energy spectra of the most energetic photon normalised to the beam energy at $\sqrt{s} = 189$ GeV and $\sqrt{s} = 192 - 202$ GeV.

The matrix element as implemented in KORALZ [36] is used to reweight the events to any TGCs values required, testing the procedure by comparing the reweighted distributions to distributions from samples generated at various values of TGCs. In all cases good agreement is observed. The main sensitivity of single-photon events to TGCs occurs at photon energies above and below those corresponding to the radiative return to the Z.

Because of azimuthal symmetry, there are two relevant observables for single-photon events, the energy and the polar angle of the photon. Both of these variables are used to perform generalised two-dimensional binned maximum likelihood fits to determine the couplings.

3 Results

3.1 Results from Single-Photon Events

One-parameter maximum likelihood fits to the couplings κ_γ and λ_γ are performed, fixing the other one to zero. The negative log-likelihood functions are shown in Figure 4. The results obtained using events selected at $\sqrt{s} = 189$ GeV are:

$$\begin{aligned} \kappa_\gamma &= 2.1^{+0.9}_{-1.0} \pm 0.4\,(68\%\,\mathrm{CL}) \\ \lambda_\gamma &= 0.6^{+1.3}_{-1.3} \pm 0.5\,(68\%\,\mathrm{CL})\,, \end{aligned}$$

where the first error is statistical and the second one is systematic. The main systematic errors for both TGCs are due to the uncertainty on the selection efficiency, the photon energy calibration and limited Monte Carlo statistics. The results obtained using events selected at $\sqrt{s} = 192 - 202$ GeV are:

$$\begin{aligned} \kappa_\gamma &= -0.7^{+0.9}_{-0.7} \pm 0.5\,(68\%\,\mathrm{CL}) \\ \lambda_\gamma &= -0.2^{+0.9}_{-0.9} \pm 0.5\,(68\%\,\mathrm{CL}). \end{aligned}$$

Combining all data taken at $\sqrt{s} = 189 - 202$ GeV yields the following 95% CL limits:

$$\begin{aligned} -1.7 &< \kappa_\gamma < 1.8 \\ -1.6 &< \lambda_\gamma < 1.7\,. \end{aligned}$$

All results quoted above are preliminary.

3.2 Results from W-pair and Single-W Events

Imposing the constraints $\Delta\kappa_Z = \Delta g_1^Z - \Delta\kappa_\gamma \tan^2\theta_w$ and $\lambda_Z = \lambda_\gamma$, the three C- and P-conserving couplings g_1^Z, κ_γ and λ_γ are fitted. The results of the one-parameter fits to all data at 189 GeV, 192 GeV, 196 GeV, 200 GeV and 202 GeV, combining W-pair and single-W measurements are:

$$g_1^Z = 0.93^{+0.05}_{-0.04} \pm 0.03 \pm 0.02 \;\; (68\%\,\mathrm{CL}),$$

$$\kappa_\gamma = 0.96^{+0.07}_{-0.07} \pm 0.09 \pm 0.04 \;\; (68\%\,\mathrm{CL}),$$

$$\lambda_\gamma = -0.08^{+0.04}_{-0.04} \pm 0.04 \pm 0.02 \;\; (68\%\,\mathrm{CL}),$$

where for each coupling the first error quoted is statistical, the second one is systematic and the third one comes from the theoretical uncertainty on the total cross section (2% for W-pair and 7% for single-W). The separate results for W-pair events collected in 1998 and 1999 and for single W events are compared in Table 1. Combination with the single-photon results reported in Sec. 3.1 does not improve the measurement of λ_γ, given the reduced sensitivity of that channel; the κ_γ result is modified to give:

$$\kappa_\gamma = 0.94^{+0.12}_{-0.11} \;\; (68\%\,\mathrm{CL}).$$

The couplings g_5^{Z}, κ_{Z} and λ_{Z} are also measured by performing single parameter fits, fixing all others to their SM values. The results obtained combining W-pair results at energies between 189 GeV and 202 GeV are:

$$g_5^{\mathrm{Z}} = -0.04^{+0.20}_{-0.21} \pm 0.12 \pm 0.06 \;\; (68\%\,\mathrm{CL}),$$

$$\kappa_{\mathrm{Z}} = 0.87^{+0.08}_{-0.07} \pm 0.08 \pm 0.04 \;\; (68\%\,\mathrm{CL}),$$
$$\lambda_{\mathrm{Z}} = -0.14^{+0.11}_{-0.06} \pm 0.08 \pm 0.05 \;\; (68\%\,\mathrm{CL}),$$

where for each coupling the first error quoted is statistical, the second one is systematic and the third one comes from the theoretical uncertainty on the total cross section (2% for W-pair and 7% for single-W). These results are also shown in Table 2, where contributions from different data sets are displayed.

The negative log-likelihood curves for the one-parameter fits are shown in Figure 5, where the contributions from W-pair events collected at $192 \leq \sqrt{s} \leq 202$ GeV and at 189 GeV and from single-W events (for electromagnetic couplings) are shown separately.

For the set of couplings g_1^{Z}, κ_γ and λ_γ, with the constraints $\Delta\kappa_{\mathrm{Z}} = \Delta g_1^{\mathrm{Z}} - \Delta\kappa_\gamma \tan^2\theta_w$ and $\lambda_{\mathrm{Z}} = \lambda_\gamma$, two- and three-parameter fits were also performed. The numerical values of the results of two-parameter fits and the correlation coefficients between the couplings are given in Table 3. In each case all couplings which are not left free to vary in the fit are set to their Standard Model value. The results of the three-parameter fit to the couplings g_1^{Z}, κ_γ and λ_γ and the correlation coefficients between them are shown in Table 4. The values quoted for the multi-parameter fits result from the combination of all data taken in 1998 and 1999, including W-pair and single-W.

Contour plots of 68% and 95% confidence level obtained from the two-parameter fits are shown in Figure 6. These contour curves correspond to a change in log-likelihood with respect to its minimum of 1.15 and 3.0, respectively. In the same figure we also plot the contours corresponding to a change in log-likelihood of 1.15 obtained from three-parameter fits; in this case the log-likelihood is minimised with respect to the third coupling.

All results are consistent with the Standard Model expectations and place limits on any anomalous contributions to the triple-gauge-boson couplings.

The fitted statistical errors agree well with the statistical errors expected for the size of the data sample used. For the W-pair results, the systematic error assigned to the couplings is dominated by the theoretical uncertainty in the total WW cross section of 2%, uncertainties in the experimental event selection efficiencies, and uncertainties in the Monte Carlo simulation of misreconstruction of the lepton and jet charges. Furthermore the assigned systematic errors take into account uncertainties in M_{W}, Γ_{W}, $\sqrt{s}$ (0.04 GeV), the measurement of the luminosity, initial and final state radiation, fragmentation and final state interactions, background normalisation and shape, and detector resolutions and energy scales. These uncertainties typically induce a shift in the minimum of the likelihood as well as a loss of sensitivity. If the increase of fit error due to a variation of one of the systematic error sources mentioned above is not balanced by a decrease of error for an opposite variation of that source, both effects are taken into account. The systematic error for 189 GeV data has been taken as a preliminary estimation for the 1999 data, except for the largest contributing sources (uncertainty in the total WW cross section and uncertainty in the Monte Carlo simulation of charge assignment), which have been tested directly.

4 Summary and Conclusions

We have studied triple-gauge-boson couplings of the W boson using data collected by the L3 detector at $\sqrt{s}$ = 189, 192, 196, 200 and 202 GeV, corresponding to a total integrated luminosity of 410 pb^{-1}. Three processes sensitive to triple gauge couplings have been analysed: $\mathrm{e^+e^-} \rightarrow \mathrm{W^+W^-}$ (W-pair production), $\mathrm{e^+e^-} \rightarrow \mathrm{We}\nu$ (single-W production) and $\mathrm{e^+e^-} \rightarrow \nu\bar{\nu}\gamma$ (single-photon production). Imposing constraints between WWZ and WWγ couplings that ensure custodial SU(2) symmetry, we have performed one-, two- and three-parameter fits to the couplings g_1^{Z}, κ_γ and λ_γ. The couplings g_5^{Z}, κ_{Z} and λ_{Z} have been measured in one-parameter fits, with no additional constraints imposed. From the 1-parameter fits, combining single-W and W-pair events, we have found

0.82	$< g_1^{\mathrm{Z}} <$	1.04
0.73	$< \kappa_\gamma <$	1.20
-0.19	$< \lambda_\gamma <$	0.05
-0.52	$< g_5^{\mathrm{Z}} <$	0.42
0.66	$< \kappa_{\mathrm{Z}} <$	1.12
-0.34	$< \lambda_{\mathrm{Z}} <$	0.16

at 95% confidence level.

In all fits, we have obtained good agreement with the SM expectations, and we have placed limits on anomalous contributions to the triple-gauge-boson couplings.

References

[1] F. Boudjema *et al.*, in *Physics at LEP 2*, Report CERN 96-01 (1996), eds G. Altarelli, T. Sjöstrand, F. Zwirner, Vol. 1, p. 207.

[2] S. L. Glashow, Nucl. Phys. **22** (1961) 579;
S. Weinberg, Phys. Rev. Lett. **19** (1967) 1264;
A. Salam, in *Elementary Particle Theory*, ed. N. Svartholm, Stockholm, Almquist and Wiksell (1968), 367.

[3] D. Bardin *et al.*, Nucl. Phys. (Proc. Suppl.) **B 37** (1994) 148;
F.A. Berends *et al.*, Nucl. Phys. (Proc. Suppl.) **B 37** (1994) 163.

[4] W. Beenakker *et al.*, in *Physics at LEP 2*, Report CERN 96-01 (1996), eds G. Altarelli, T. Sjöstrand, F. Zwirner, Vol. 1, p. 79.

[5] D. Bardin *et al.*, in *Physics at LEP 2*, Report CERN 96-01 (1996), eds G. Altarelli, T. Sjöstrand, F. Zwirner, Vol. 2, p. 3.

[6] K. Hagiwara, R.D. Peccei, D. Zeppenfeld and K. Hikasa, Nucl. Phys. **B 282** (1987) 253.

[7] K. Gaemers and G. Gounaris, Z. Phys. **C 1** (1979) 259.

[8] M. Bilenky, J.L. Kneur, F.M. Renard and D. Schildknecht, Nucl. Phys. **B 409** (1993) 22; Nucl. Phys. **B 419** (1994) 240.

[9] I. Kuss and D. Schildknecht, Phys. Lett. **B 383** (1996) 470.

[10] G. Gounaris *et al.*, in *Physics at LEP 2*, Report CERN 96-01 (1996), eds G. Altarelli, T. Sjöstrand, F. Zwirner, Vol. 1, p. 525.

[11] The L3 Collaboration, M. Acciarri *et al.*, Phys. Lett. **B 398** (1997) 223.

[12] The L3 Collaboration, M. Acciarri *et al.*, Phys. Lett. **B 413** (1997) 176.

[13] The L3 Collaboration, M. Acciarri *et al.*, *Preliminary Results on the Measurement of Triple-Gauge-Boson Couplings of the W Boson at LEP*, L3 Note 2378.

[14] The L3 Collaboration, M. Acciarri *et al.*, *Production of Single W Bosons at $\sqrt{s}$ = 189 GeV and Measurement of WWγ Gauge Couplings*, L3 preprint 212, submitted to Physics letters B.

[15] The L3 Collaboration, M. Acciarri *et al.*, *Preliminary Results on Single W Boson Production at 192 GeV $\leq \sqrt{s} \leq$ 202 GeV*, L3 Note 2518 (2000).

[16] The L3 Collaboration, B. Adeva *et al.*, Nucl. Instr. and Meth. **A 289** (1990) 35;
M. Chemarin *et al.*, Nucl. Instr. and Meth. **A 349** (1994) 345;
M. Acciarri *et al.*, Nucl. Instr. and Meth. **A 351** (1994) 300;
G. Basti *et al.*, Nucl. Instr. and Meth. **A 374** (1996) 293;
I.C. Brock *et al.*, Nucl. Instr. and Meth. **A 381** (1996) 236;
A. Adam *et al.*, Nucl. Instr. and Meth. **A 383** (1996) 342.

[17] The L3 Collaboration, M. Acciarri *et al.*, *Preliminary results on the Measurement of W-Pair Cross Sections in* e^+e^- *Interactions at* $\sqrt{s} = 192 - 202$ *GeV and W-Decay Branching Fractions*, L3 Note 2514.

[18] The L3 Collaboration, M. Acciarri *et al.*, Phys. Lett. **B 407** (1997) 419.

[19] The KORALW version 1.33 is used.
M. Skrzypek, S. Jadach, W. Placzek and Z. Wąs, Comp. Phys. Comm. **94** (1996) 216;
M. Skrzypek, S. Jadach, M. Martinez, W. Placzek and Z. Wąs, Phys. Lett. **B 372** (1996) 289.

[20] The HERWIG version 5.9 is used.
G. Marchesini and B. Webber, Nucl. Phys. **B 310** (1988) 461;
I.G. Knowles, Nucl. Phys. **B 310** (1988) 571;
G. Marchesini *et al.*, Comp. Phys. Comm. **67** (1992) 465.

[21] F.A. Berends, R. Kleiss and R. Pittau, Nucl. Phys. **B 424** (1994) 308; Nucl. Phys. **B 426** (1994) 344; Nucl. Phys. (Proc. Suppl.) **B 37** (1994) 163;
R. Kleiss and R. Pittau, Comp. Phys. Comm. **83** (1994) 141;
R. Pittau, Phys. Lett. **B 335** (1994) 490.

[22] PYTHIA version 5.722 is used.
T. Sjöstrand, *PYTHIA 5.7 and JETSET 7.4 Physics and Manual*,
CERN-TH/7112/93 (1993), revised August 1995; Comp. Phys. Comm. **82** (1994) 74.

[23] The KORALZ version 4.01 is used.
S. Jadach, B. F. L. Ward and Z. Wąs, Comp. Phys. Comm. **79** (1994) 503.

[24] J.H. Field, Phys. Lett. **B 323** (1994) 432;
J.H. Field and T. Riemann, Comp. Phys. Comm. **94** (1996) 53.

[25] BHWIDE version 1.01 is used.
S. Jadach, W. Placzek, B.F.L. Ward, Phys. Rev. **D 40** (1989) 3582, Comp. Phys. Comm. **70** (1992) 305, Phys. Lett. **B 390** (1997) 298.

[26] D. Karlen, Nucl. Phys. **B 289** (1987) 23.

[27] F. A. Berends, P. H. Daverfeldt and R. Kleiss, Nucl. Phys. **B 253** (1985) 441.

[28] J.A.M. Vermaseren, J. Smith and G. Grammer Jr, Phys. Rev. **D 19** (1979) 137;
J.A.M. Vermaseren, Nucl. Phys. **B 229** (1983) 347.

[29] PHOJET version 1.05 is used.
R. Engel, Z. Phys. **C 66** (1995) 203; R. Engel and J. Ranft, Phys. Rev. **D 54** (1996) 4244.

[30] The L3 detector simulation is based on GEANT Version 3.15.
R. Brun *et al.*, *GEANT 3*, CERN-DD/EE/84-1 (Revised), 1987.
The GHEISHA program (H. Fesefeldt, RWTH Aachen Report PITHA 85/02 (1985)) is used to simulate hadronic interactions.

[31] The UA1 Collaboration, C. Albajar *et al.*, Z. Phys. **C 44** (1989) 15;
The UA2 Collaboration, J. Alitti *et al.*, Phys. Lett. **B 241** (1990) 150; Phys. Lett. **B 276** (1992) 354;
The CDF Collaboration, F. Abe *et al.*, Phys. Rev. Lett. **65** (1990) 2243; Phys. Rev. **D 43** (1991) 2070; Phys. Rev. Lett. **75** (1995) 11; Phys. Rev. **D 52** (1995) 4784;
The DØ Collaboration, S. Abachi *et al.*, Phys. Rev. Lett. **77** (1996) 3309.
We use the average value and error for the mass of the W boson as listed in:
R.M. Barnett *et al.*, *Review of Particle Properties*, Phys. Rev. **D 54** (1996) 1.

[32] R.D. Field, R.P. Feynman, Nucl. Phys. **B 136** (1978) 1.

[33] P. Fisher, *Polar angle determination in* WW $\rightarrow$ *4 jet events*, L3 Note 2221 (1998).

[34] D.M. Schmidt, R.J. Morrison and M.S. Witherell, Nucl. Instr. and Meth. **A 328** (1993) 547.

[35] The L3 Collaboration, M. Acciarri *et al.*, Phys. Lett. **B470** (1999) 268.

[36] S. Jadach, B. F. L. Ward and Z. Wąs, Comp. Phys. Comm. **79** (1994) 503.

Fit par.	WW 98	WW 99	Single W	All data combined	
				68% CL	95% CL
g_1^{Z}	$1.00^{+0.08}_{-0.08} \pm 0.04$	$0.89^{+0.05}_{-0.05} \pm 0.04$	-	$0.93^{+0.06}_{-0.05}$	(0.82; 1.04)
κ_γ	$0.81^{+0.17}_{-0.14} \pm 0.15$	$0.83^{+0.11}_{-0.09} \pm 0.11$	$1.08^{+0.14}_{-0.15}$	$0.96^{+0.12}_{-0.12}$	(0.73; 1.20)
λ_γ	$-0.01^{+0.08}_{-0.08} \pm 0.05$	$-0.12^{+0.05}_{-0.05} \pm 0.05$	$0.12^{+0.27}_{-0.42}$	$-0.08^{+0.06}_{-0.06}$	(-0.19; 0.05)

Table 1: Results of one-parameter fits to the triple-gauge-boson couplings g_1^{Z}, κ_γ and λ_γ with the constraints $\Delta\kappa_{\mathrm{Z}} = \Delta g_1^{\mathrm{Z}} - \Delta\kappa_\gamma \tan^2\theta_w$ and $\lambda_{\mathrm{Z}} = \lambda_\gamma$ imposed. The first two columns show results obtained from W-pair events collected at centre-of-mass energies of 189 GeV and 192-202 GeV during 1998 and 1999. The third column shows the results derived from single W events collected at the same energies after removing the events which were already selected as WW. The last two columns contain the results obtained combining WW and single-W measurements, at 68% CL and at 95% CL. In the first two columns statistical and systematic errors are shown separately; in the rest of the table they are combined.

Fit par.	WW 98	WW 99	All data combined	
			68% CL	95% CL
g_5^{Z}	$0.15^{+0.32}_{-0.32} \pm 0.16$	$-0.17^{+0.26}_{-0.26} \pm 0.15$	$-0.04^{+0.24}_{-0.25}$	(-0.52; 0.42)
κ_{Z}	$0.99^{+0.15}_{-0.14} \pm 0.10$	$0.82^{+0.09}_{-0.08} \pm 0.10$	$0.87^{+0.12}_{-0.11}$	(0.66; 1.12)
λ_{Z}	$0.02^{+0.15}_{-0.15} \pm 0.10$	$-0.21^{+0.09}_{-0.08} \pm 0.10$	$-0.14^{+0.14}_{-0.11}$	(-0.34; 0.16)

Table 2: Results of the one-parameter fits to the triple-gauge-boson couplings g_5^{Z}, κ_{Z} and λ_{Z} with no additional constraints imposed, all other couplings being set to their Standard Model value. The first two columns show results obtained from W-pair events collected at centre-of-mass energies of 189 GeV and 192-202 GeV during 1998 and 1999; statistical and systematic errors are shown separately. The third and fourth columns contain the combined results, including systematic errors, at 68% CL and at 95%CL.

2-parameter fits			
Fit parameter	Other parameters	Results (68% CL)	Results (95% CL)
g_1^{Z}	$\lambda_\gamma = 0$	$0.96^{+0.06}_{-0.11}$	$0.79 < g_1^{\mathrm{Z}} < 1.08$
κ_γ		$0.94^{+0.26}_{-0.10}$	$0.74 < \kappa_\gamma < 1.33$
		cor = -0.40	
g_1^{Z}	$\kappa_\gamma = 0$	$0.99^{+0.11}_{-0.15}$	$0.74 < g_1^{\mathrm{Z}} < 1.18$
λ_γ		$-0.07^{+0.17}_{-0.11}$	$-0.25 < \lambda_\gamma < 0.24$
		cor = -0.83	
κ_γ	$g_1^{\mathrm{Z}} = 0$	$1.04^{+0.11}_{-0.19}$	$0.74 < \kappa_\gamma < 1.28$
λ_γ		$-0.09^{+0.11}_{-0.06}$	$-0.21 < \lambda_\gamma < 0.05$
		cor = -0.13	

Table 3: Results of two-parameter fits to the triple-gauge-boson couplings g_1^{Z}, κ_γ and λ_γ, with the constraints $\Delta\kappa_{\mathrm{Z}} = \Delta g_1^{\mathrm{Z}} - \Delta\kappa_\gamma \tan^2\theta_w$ and $\lambda_{\mathrm{Z}} = \lambda_\gamma$ imposed. These results are obtained from the combination of W-pair and single-W data taken at energies between 189 GeV and 202 GeV. Systematic errors are included.

3-parameter fit			correlation coefficients			
Fit parameter	Results (68% CL)	Results (95% CL)		g_1^{Z}	κ_γ	λ_γ
g_1^{Z}	$0.97^{+0.12}_{-0.15}$	$0.72 < g_1^{\mathrm{Z}} < 1.18$	g_1^{Z}	1.00	-0.36	-0.67
κ_γ	$1.06^{+0.13}_{-0.21}$	$0.74 < \kappa_\gamma < 1.33$	κ_γ		1.00	0.12
λ_γ	$-0.06^{+0.16}_{-0.11}$	$-0.26 < \lambda_\gamma < 0.24$	λ_γ			1.00

Table 4: Results of the three-parameter fit to the triple-gauge-boson couplings g_1^{Z}, κ_γ and λ_γ, with the constraints $\Delta\kappa_{\mathrm{Z}} = \Delta g_1^{\mathrm{Z}} - \Delta\kappa_\gamma \tan^2\theta_w$ and $\lambda_{\mathrm{Z}} = \lambda_\gamma$ imposed. This result is obtained from the combination of W-pair and single-W data taken at energies between 189 GeV and 202 GeV. Systematic errors are included. The correlation matrix is also shown.

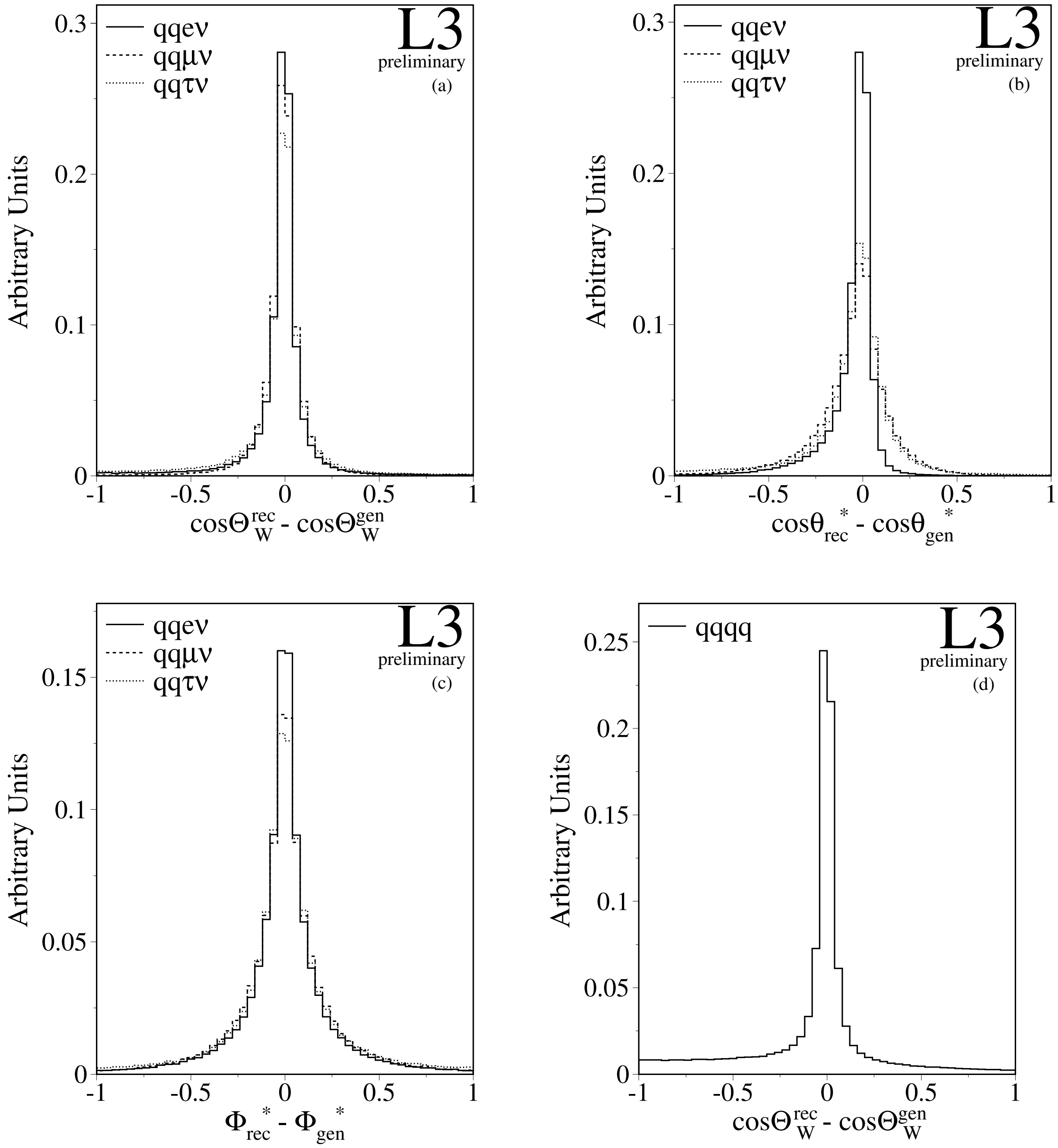

Figure 1: Monte Carlo predictions of the resolutions in the reconstruction of the phase space angles $\Theta_{\rm W}$ (a), Θ_l^* (b), and ϕ_l^* (c) for $qq\ell\nu$ events, and $\Theta_{\rm W}$ (d) for $qqqq$ events.

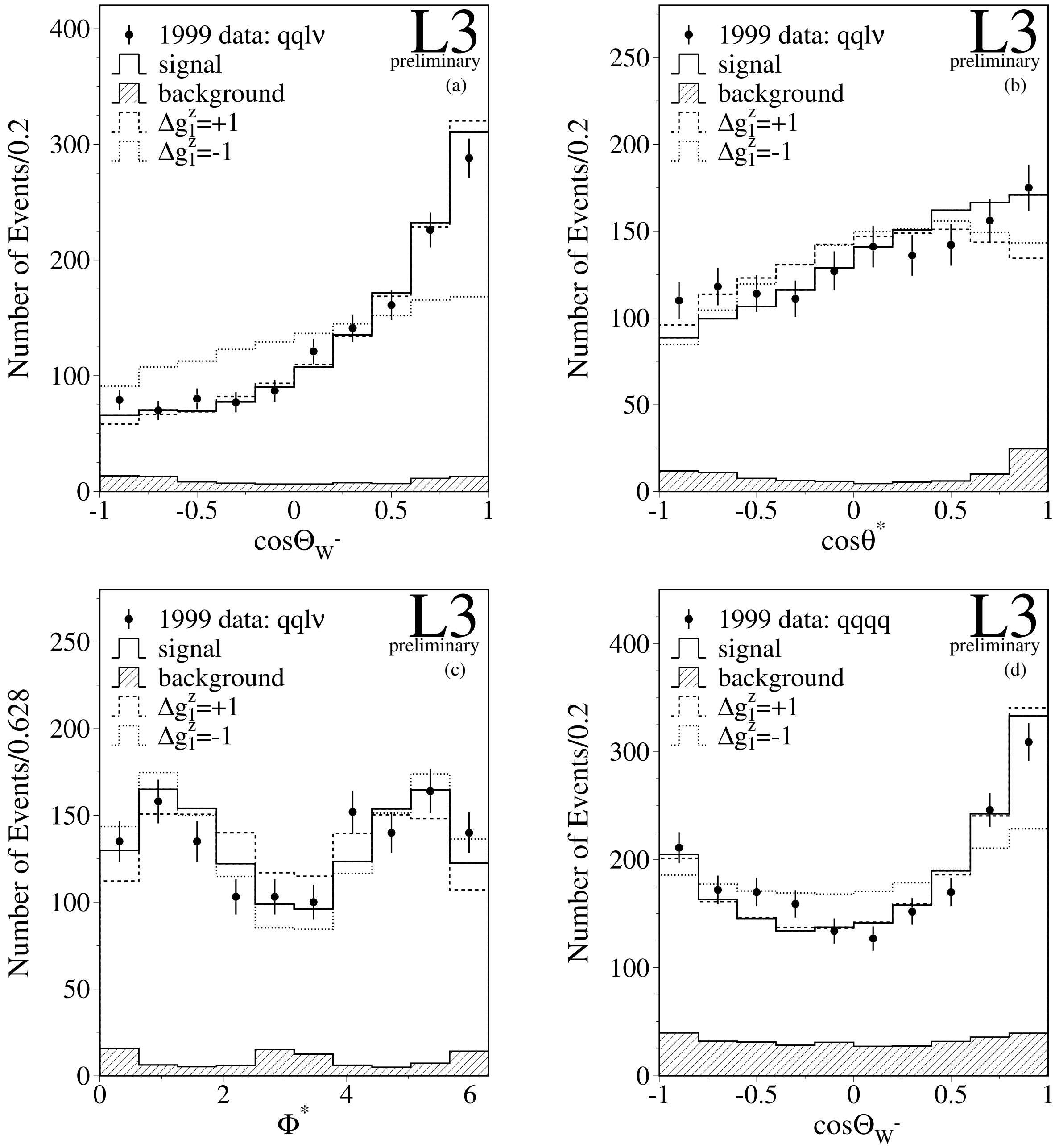

Figure 2: Distributions of the phase space angles in selected data events at 192-202 GeV: $\cos\Theta_{\mathrm{W}}$ (a), $\cos\theta_l^*$ (b) and ϕ_l^* (c) for $qq\ell\nu$ events, and $\cos\Theta_{\mathrm{W}}$ (d) for $qqqq$ events. Open histograms show the Monte Carlo signal predictions, dashed histograms the background. As an example of the effects of anomalous couplings, distributions of these phase space angles for $\Delta g_1^{\mathrm{Z}} = \pm 1$, normalized to the SM prediction, are shown as well. In (c), the ϕ_l^* distribution for W^- decays is shifted by π in order to have the same ϕ_l^* distribution for W^- and W^+ decays.

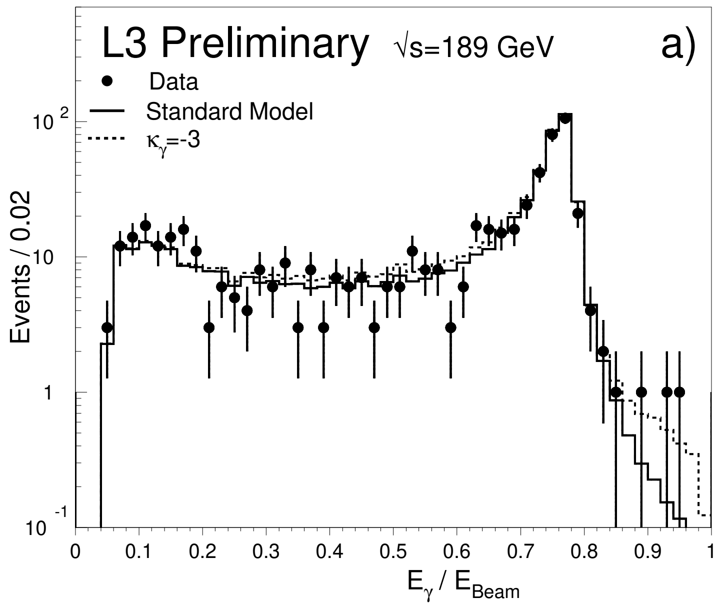

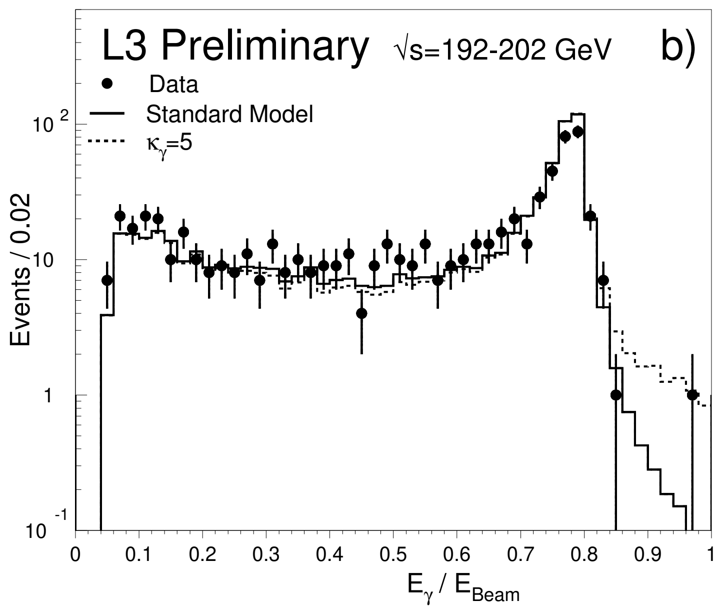

Figure 3: Energy of the highest energetic photon normalised to the beam energy for single-photon events selected at (a) $\sqrt{s} = 189$ GeV and (b) $\sqrt{s} = 192 - 202$ GeV. The expectations for anomalous TGCs (dashed line) are shown as well.

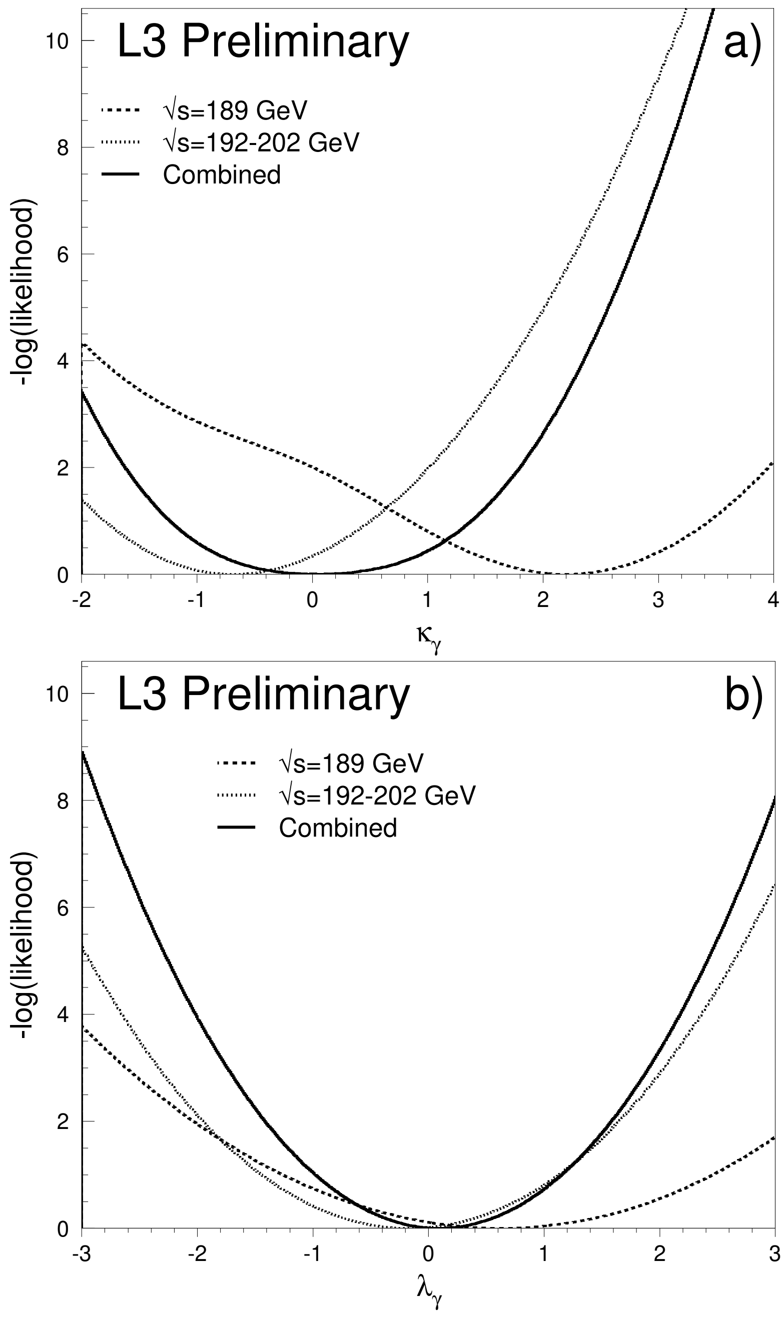

Figure 4: Negative log-likelihood curves for one parameter fits to the the couplings κ_γ (a) and λ_γ(b). The two dashed lines correspond to likelihoods obtained using single-photon events selected at $\sqrt{s} = 189$ GeV and $\sqrt{s} = 192 - 202$ GeV. The solid line is the combined likelihood curve.

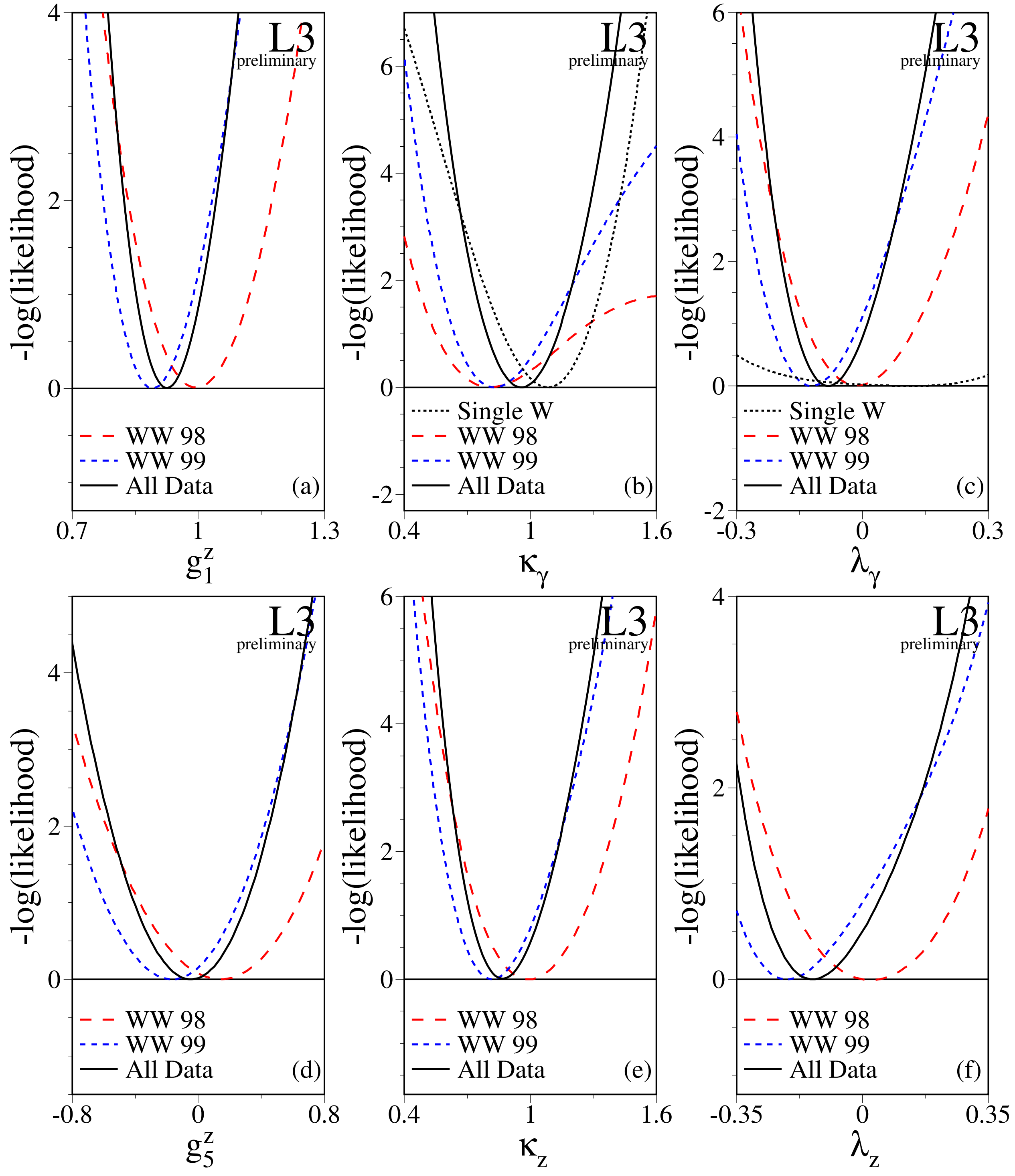

Figure 5: Negative log-likelihood curves for one-parameter fits to the couplings g_1^Z (a), κ_γ (b), λ_γ (c), with the constraints $\Delta\kappa_Z = \Delta g_1^Z - \Delta\kappa_\gamma \tan^2\theta_w$ and $\lambda_Z = \lambda_\gamma$, and g_5^Z (d), κ_Z (e) and λ_Z (f) with no additional constraints imposed. The contributions from W-pair events collected at $192 \leq \sqrt{s} \leq 202$ GeV is added to the one obtained from 1998 data at 189 GeV; for electromagnetic couplings (κ_γ and λ_γ) also the single-W contribution is plotted. Systematic errors are taken into account.

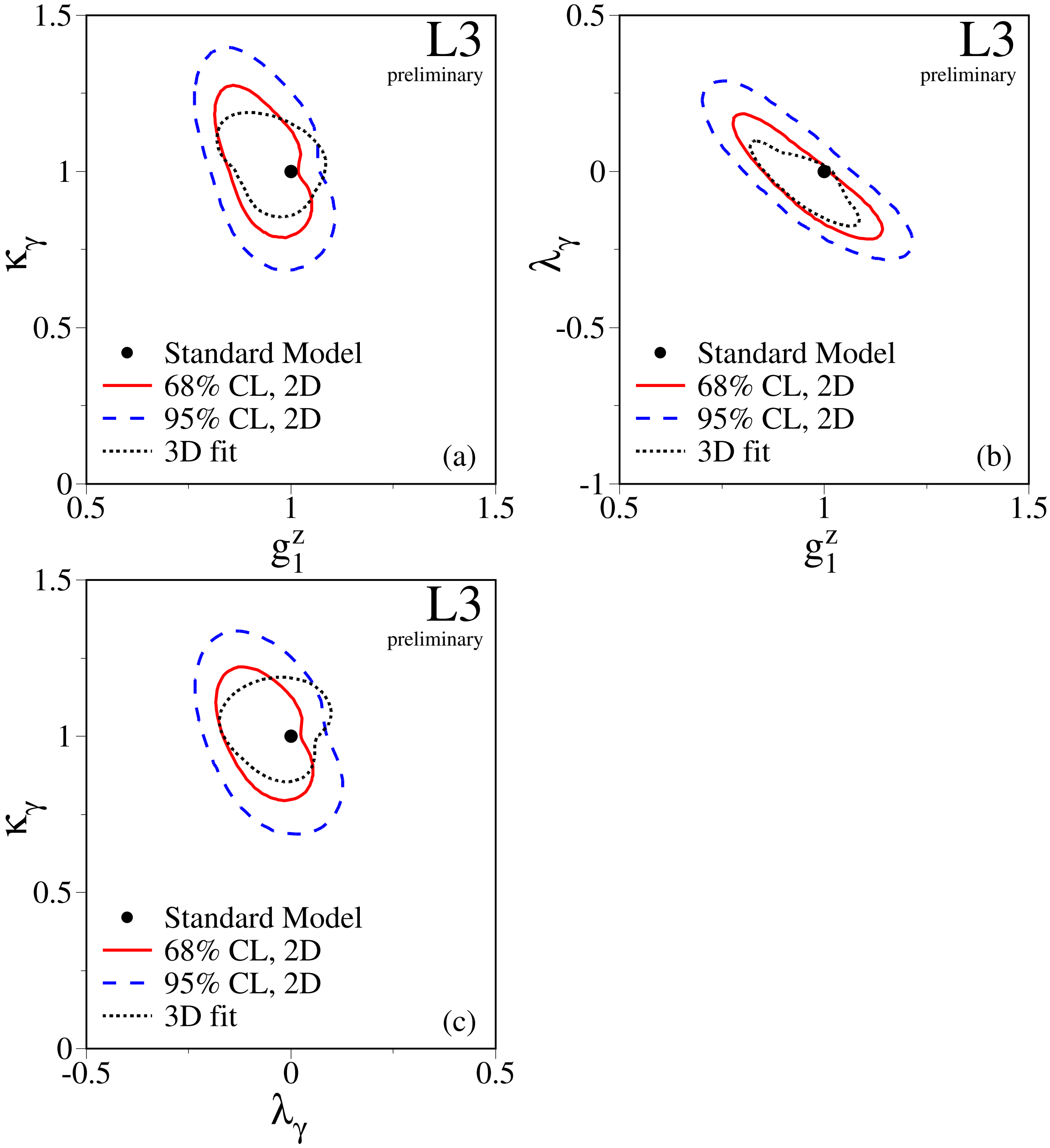

Figure 6: 68%(full line) and 95%(dashed line) confidence level contour curves for two-parameter fits to the couplings κ_γ and g_1^Z (with $\lambda_\gamma = 0$) (a), λ_γ and g_1^Z (with $\kappa_\gamma = 0$) (b), λ_γ and κ_γ (with $g_1^Z = 0$) (c). The dotted contours are obtained from three-parameter fits by requiring a log-likelihood change of 1.15 with respect to the minimum, and minimising at each point with respect to the third coupling. These contours are obtained using all the data from 1998 and 1999, combining single-W and W-pair events, and taking systematic errors into account. The constraints $\Delta\kappa_Z = \Delta g_1^Z - \Delta\kappa_\gamma \tan^2\theta_w$ and $\lambda_Z = \lambda_\gamma$ are imposed.